ELSEVIER

Polymer 41 (2000) 6955–6964

polymer

Polymer Communication

In situ resonant Raman and optical investigations of p-doped poly (*p*-phenylene vinylene)

M. Baïtoul[a,b], J. Wéry[a,*], J.-P. Buisson[a], G. Arbuckle[c], H. Shah[1,c], S. Lefrant[a], M. Hamdoume[b]

[a]*Laboratoire de Physique Cristalline, Institut des Matériaux Jean Rouxel, UMR 6502, Université de Nantes, 2 rue de la Houssinière, BP 32229, 44322 Nantes, Cedex 3, France*

[b]*Laboratoire de Physique du Solide, Faculté des Sciences de Fès 30.000, Morocco*

[c]*Department of Chemistry, Rutgers University, Camden, NJ 08102, USA*

Received 19 May 1999; received in revised form 29 December 1999; accepted 6 January 2000

Abstract

In this paper, we present spectroscopy studies of poly (*p*-phenylene vinylene) p-doped by chemical or electrochemical ways with SO_3^- and BF_4^-, respectively. Since very few experimental data are available for in situ Raman studies of electrochemically doped samples, we have essentially used this technique in different resonance conditions (resonance Raman scattering (RRS)) to carry out our investigations using different excitation wavelengths. Several modifications in the Raman spectra of doped PPV compared to neutral PPV are analyzed and interpreted by the coexistence of polaronic and bipolaronic species in the sample. These results are illustrated in particular by gradual shifts in the frequency of carbon–carbon stretching vibrations, explained in terms of a quinoid character growing at the expense of the benzenoid one when the doping level is increased.

Keywords: Electrochemical studies; Raman spectroscopy; Optical spectroscopy

1. Introduction

Conjugated polymers have attracted interest, in both fundamental and applied research due to the numerous possibilities identified for their potential use in electronics, optoelectronics and non-linear optics [1,2]. Much of this interest originates from the discovery that the electrical conductivity of such compounds can be varied from an initially insulating state to a highly conducting state after doping with electron donors (n-type doping) or acceptors (p-type doping) [3–6]. PPV and substituted derivatives are nowadays extensively studied for the reasons mentioned above. Therefore, it is of particular interest to study the changes of the electronic structure upon doping. Such investigation has been carried out in our laboratory for n-doped PPV [7,8]. Let recall that the main objective of structural studies is to elucidate the relationship between the electrical conduction and the modifications of the electronic distribution on the polymer backbone occurring after doping. The resonant Raman spectroscopy is one of the tools which is used to probe such modifications on an intrachain scale after chemical or electrochemical doping. Since PPV has a non-degenerate ground state, the modifications obtained upon doping have been discussed in terms of polarons and bipolarons. These excitations which have charge and/or spin are associated with geometric deformations along the polymeric chain referred to a quinoid type of structure as theoretically established [9].

The purpose of this study is to describe at an intrachain scale the structural modifications induced by such charged defects. As a matter of fact, the only results available in the literature are related to limited Raman data when PPV samples are electrochemically doped. For example, PPV doped with AsF_6^- was studied with UV–visible absorption and FTIR spectroscopies [10] or EPR and conductivity in the case of a derivative polymer of PPV doped with BF_4^- [11]. Other reports can be found (see, for example Ref. [12]), but very little deal with Raman spectroscopy. For these reasons, we focused our work on resonance Raman scattering (RRS) on electrochemically p-doped PPV, whereas studies of chemically doped samples are presented for comparison purpose. The effects of the electrochemical oxidative doping have been investigated in a parallel way by in situ optical absorption and resonant Raman spectroscopy. As a matter of fact, the electrochemical method of oxidation is advantageous for studying doping-induced changes in the

* Corresponding author.

[1] Permanent address: Department of Chemistry, Clemson University, Clemson, SC 29634, USA.

0032-3861/00/$ - see front matter
PII: S0032-3861(00)00022-7

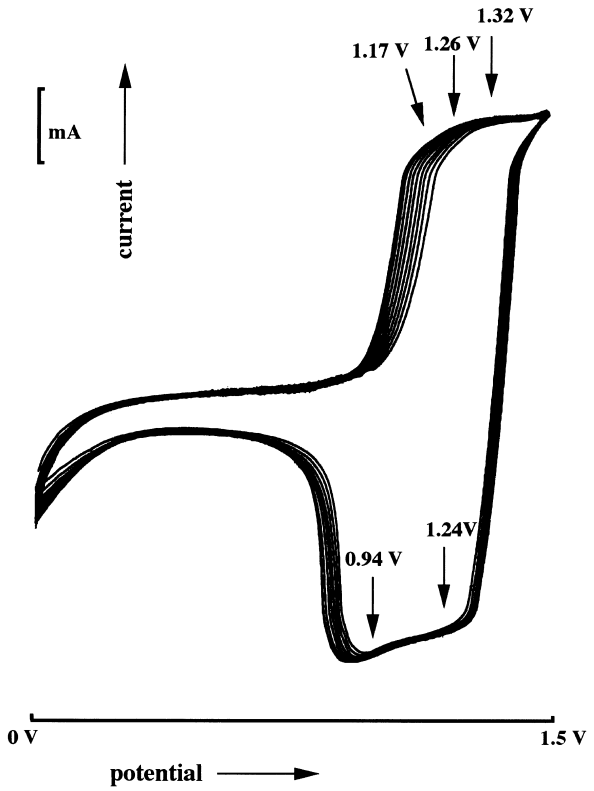

Fig. 1. Cyclic voltammograms of PPV with 0.2 M $TBABF_4$ solution in acetonitrile (reference Ag/Ag^+; scan rate: 20 mV/s).

electronic structure of the polymer in a gradual and reversible way, in particular from the analysis of the Raman spectra of p-doped PPV. In addition, since resonance conditions are specific to the absorption of different species, we can observe the enhancement of some Raman bands associated to them. As expected, the modifications observed in the Raman spectra are explained in terms of a quinoid structure growing at the expense of the benzenoid one. In addition, we report for comparison Raman spectra of SO_3 doped PPV taken at different excitation wavelengths. From our experimental data, we deduce information about the nature of the chemical bonds with respect to the neutral polymer. Let us recall that the doped PPV polymer has been investigated by in situ X-ray diffraction studies limited to oriented samples doped with Na in vapor phase [13]. To our knowledge, no structural data are available on PPV doped electrochemically. Therefore, our Raman studies can provide real insight on the chemical modifications occurring on the chains after doping.

2. Experimental details

PPV films have been prepared in our laboratory by using a soluble precursor polymer, containing tetrahydrothiophenium group [14], according to a procedure published previously by Wessling et al. [15]. This precursor polymer, which exhibits improved properties such as solubility in organic solvents (methanol), was thermally converted to PPV. In order to carry out spectroscopic investigations, the precursor polymer solution is deposited onto a platinum electrode whenever Raman scattering experiments are performed and on a transparent electrode coated with indium tin oxide (ITO) for optical absorption measurements. Then, the obtained thin film is converted into PPV at a typical temperature of 250°C under dynamic secondary vacuum ($\sim 10^{-6}$ Torr) for a duration of $\sim$3 h. An electrochemical cell, with three electrodes, is used for all in situ studies in a configuration using the converted polymer as the working electrode, together with a platinum counter electrode, and a reference one (Ag/Ag^+). An appropriate electrolyte in a solvent with a range of electrochemical activity consistent with the oxidation potential of the polymer is used, such as tetrabutylammonium tetrafluoroborate ($TBABF_4$) solution in acetonitrile (0.2 M) in this study.

In the case of SO_3^- doped PPV, unstretched films were doped by exposure to SO_3 vapor under vacuum. According to the duration of the exposure, different stages of doping have been qualitatively obtained and the samples obtained have been labelled lightly doped, highly doped and overdoped, respectively. SO_3^- doped PPV are highly air sensitive and so, they were stored in a vacuum sealed tube for spectroscopic measurements.

Room temperature optical absorption spectra were carried out with a double beam spectrophotometer Cary 2300 in the spectroscopy range 200–1600 nm.

Resonant Raman spectra have been recorded with different laser lines in the visible range, especially $\lambda_{exc} =$ 676.4 nm, on a multichannel Jobin-Yvon T 64000 spectrometer equipped with a cooled CCD detector. The scattering signal was collected either at 90° in macro configuration or in backscattering under microscope. When using the excitation at $\lambda_{exc} = 1064$ nm, a FT-Raman Bruker RFS 100 in backscattering configuration was used. Raman spectra were recorded with a resolution of 2 cm^{-1}. Infrared absorption experiments were performed on a Nicolet 20SXC Fourier transform spectrometer with an energy resolution of 4 cm^{-1}.

3. Results and discussion

3.1. Electrochemical oxidative doping

3.1.1. Cyclic voltammetry

Cyclic voltammograms between 0 and 1.5 V show a broad oxidation wave between 1.17 and 1.32 $V/Ag/Ag^+$ with 20 mV/s scan rate. The maximum current occurs at 1.26 $V/Ag/Ag^+$. A reversible reduction wave with two maxima is observed at 1.24 and 0.94 V, respectively (Fig. 1). $Q_{extracted}/Q_{inserted}$ is estimated to be about 80%, indicating a high degree of electrochemical reversibility. The slow oxidation process can presumably originate from the

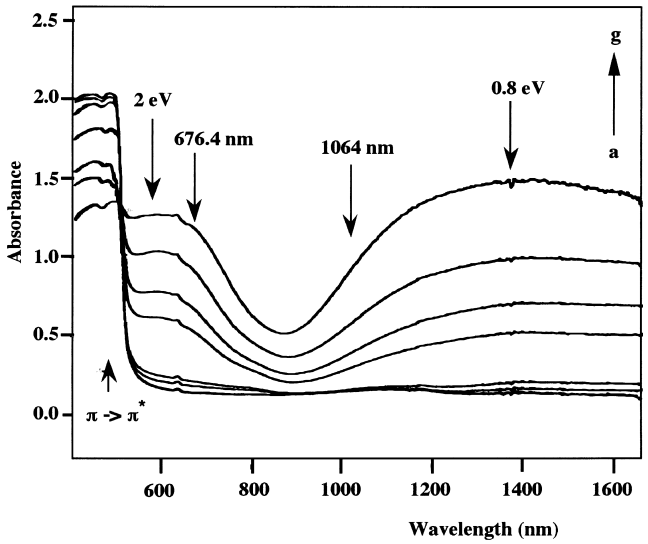

Fig. 2. Optical absorption spectra of PPV carried out in 0.2 M $TBABF_4$ solution in acetonitrile at different oxidative potentials: (a) 0 V; (b) 1 V; (c) 1.1 V; (d) 1.2 V; (e) 1.225 V; (f) 1.275 V; (g) 1.3 V.

structural arrangement induced by the dispersion of conjugation length. Indeed, the obstacle in the insertion of the iodine in PPV has been related to the state of order in this polymer [16]. In fact, we observed absolutely no degradation of the polymer up to 30 cycles. Also, cyclic voltammograms are superposed after about 15 cycles, indicating that an equilibrium has been reached in the sample.

In contrast, cyclic voltammograms obtained with lithium perchlorate in acetonitrile, between 0 and 1.30 V show a reversible oxidation wave and the onset of an irreversible one [17,18]. The oxidation onset shifts towards higher potential at values lower than those found with BF_4^-. This would indicate that side reactions occur more easily with ClO_4^- than with BF_4^-. Therefore, in the case of ClO_4^-, one cannot accurately study the reversible process. The presence of an irreversible reaction after the first reversible oxidation wave is characteristic of most conducting polymers [15]. Such behavior has been explained for many conducting polymers such as polythiophene, polyacetylene, and polyparaphenylene by an overoxidation which depends on different parameters: electrolyte, oxygen presence, etc. [19]. In order to avoid any degradation, the potential applied for all the following measurements is limited to the reversible oxidation wave.

3.1.2. In situ optoelectrochemical spectroscopy

The optical absorption spectrum of the cell containing the electrolyte is recorded without the sample in the same conditions for reference and has been subtracted from all optical absorption spectra of the PPV film after oxidation.

The modifications obtained, upon in situ electrochemical doping with BF_4^-, in optical absorption are shown in Fig. 2. The changes begin at a potential which coincides approximately with the onset of the oxidation wave in the cyclovoltammogram. As the potential increases, we observe two new bands associated with localised states whose maximum energies are around 2 eV (640 nm) and 0.8 eV (1340 nm). They are correlated with a gradual decrease of the $\pi \rightarrow \pi^*$ transition intensity whose maximum is at 2.7 eV (457 nm). The intensity of the absorption band of neutral segments decreases but its main features (energy, shape) are not modified. These results are similar to those obtained previously by Bradley et al. [20] and Schlenoff et al. [21]. On the basis of the optical absorption spectra analysis, these authors have suggested the existence of bipolarons in electrochemically oxidized PPV. In addition, other methods of p-type doping [12] or photoexcitation above the gap edge have given similar absorption bands [22]. The modifications observed during doping are consistent with an increase of the concentration of doped segments with the doping level and a decrease of the concentration of neutral chains. After dedoping, all theses features are removed with no modification in the threshold absorption of the neutral PPV, indicating a reversible origin in the charge transfer reaction. So, we have identified absorption bands associated with different charged species which we want to characterize by studying their vibrational properties.

3.1.3. In situ resonant Raman scattering

Resonant Raman spectra have been recorded with excitation lines in the visible ($\lambda_{exc} = 676.4$ nm) and the near infrared ($\lambda_{exc} = 1064$ nm) which are close in energy to electronic transitions of doped segments in order to fulfil resonance conditions for the different species induced by doping. In situ electrochemical doping shows different modifications of the Raman spectra as a function of the doping level and the excitation wavelength (Figs. 3 and 4). The Raman spectra obtained with 676.4 and 1064 nm at high doping level (1.30 V) close to the maximum of the oxidation wave in the cyclovoltammogram of BF_4^- doped PPV are shown in Fig. 5. We observe different bands whose intensities depend on the excitation wavelength indicating a resonance behavior. Notice that the main features of the Raman spectra are similar to those of ClO_4^- doped PPV [18]. Raman bands due to the solvent are clearly identified and since they are not at the frequencies characteristic of the polymer, they do not present any inconvenience. Since, in previous studies, most of the vibrational modes of neutral PPV [8,23] and p-doped PPV have been correctly assigned, the structural modifications which may occur after doping can be followed.

The present analysis does not take into account the dispersion of conjugation lengths in the polymer. Indeed, this is a difficult task since frequencies of the Raman modes are independent of the polymer length. However, recent studies [24] report the determination of distribution of conjugated lengths in neutral PPV, via the analysis of the Raman band intensities. Concerning doped samples in which charge carriers are injected, polaronic and/or bipolaronic species are expected and described in terms of

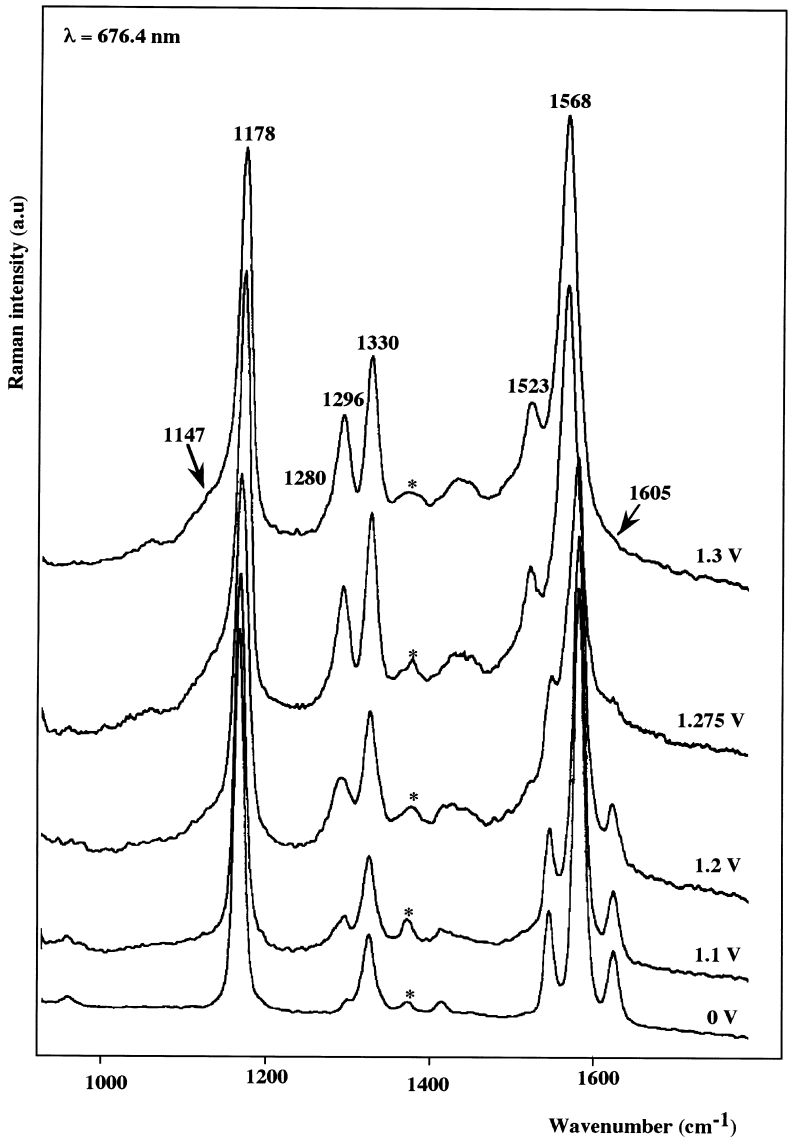

Fig. 3. Raman spectra of PPV carried out in 0.2 M $TBABF_4$ solution in acetonitrile at different oxidative potentials with laser excitation line 676.4 nm; (∗:solvent).

local distortions of the polymer backbone. They have been studied theoretically by Bredas [9], discussed through Raman studies [8] and extended in this paper to PPV samples p-doped electrochemically. To come back to the Raman analysis of our doped samples, we observe that the main changes occur in the 1500–1700 cm^{-1} range. In particular, the intensity of the band obtained at 1625 cm^{-1}, which is mainly, assigned to the stretching mode of the CC bond of the vinyl group in neutral PPV [8,23], decreases regularly upon doping. Let notice that the vibrational modes in the vinyl group are coupled to those originating from the rings. The Raman frequencies and their assignments of neutral PPV are given in Table 1.

In the 676.4 nm-excited Raman spectra (Fig. 4), at high doping level, the band observed at 1568 cm^{-1} and the very weak shoulder at ~1605 cm^{-1} are assigned to the vinyl CC stretching vibration and the ring CC stretching vibration of doped segments. This band and its additional shoulder, according to Ref. [8], originate from the neutral PPV modes located at 1625 and 1582 cm^{-1}, with some partial inversion of assignments in terms of ring and vinyl group contribution. The next band at 1523 cm^{-1}, which is assigned to the ring CC stretching vibration in doped segments, originates from the neutral PPV mode at 1546 cm^{-1}. Lefrant et al. [25] obtained a similar behavior in $FeCl_3$ doped PPV, and attributed such shifts to a distortion of the polymeric chain leading partially to a quinoid structure. The band observed at 1330 cm^{-1}, which can be interpreted as stemming from the neutral PPV mode at 1327 cm^{-1}, is assigned to a bending mode CC–H of the vinyl group. This band is slightly affected by doping. We notice that the corresponding band studied also in model compounds show relatively small

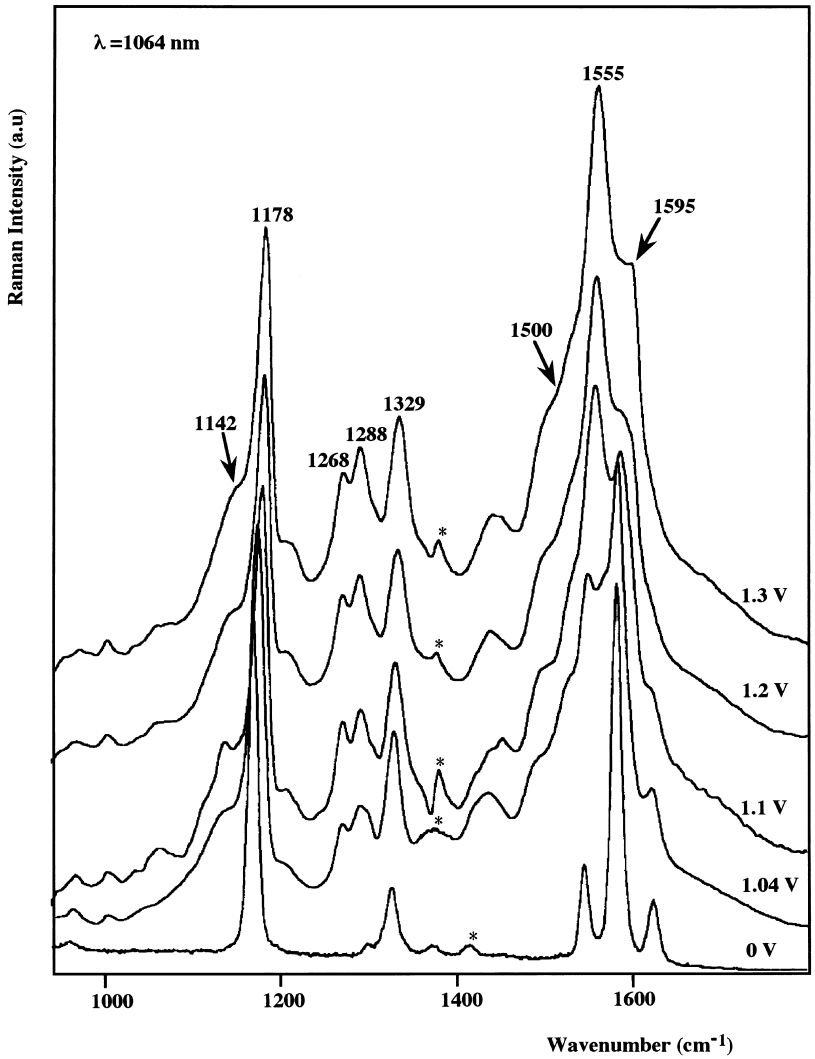

Fig. 4. Raman spectra of PPV carried out in 0.2 M $TBABF_4$ solution in acetonitrile at different oxidative potentials with laser excitation line 1064 nm; (∗:solvent).

downshifts when the length of the compound increases [8,23]. Therefore, this mode is only slightly sensitive to the electronic distribution modification. On the contrary, vibrational modes which are coupled to the π electron system are very sensitive to these modifications. The band observed at 1296 cm^{-1} and the shoulder peaked about 1280 cm^{-1} are presumably assigned to the interring CC stretching vibrations in doped segments, if one refers to those located at 1300 and 1197 cm^{-1} in neutral PPV [8]. The strong band observed at 1178 cm^{-1} originates from a shift of the same vibrational mode observed at 1170 cm^{-1} in compounds with aromatic rings. These modes are assigned to a bending mode CC–H of the ring in doped and neutral segments of PPV, respectively. Concerning the weak band recorded at 1147 cm^{-1}, only observed in model compounds [8,23], it can be assigned to a vinylene and ring CC–H bending vibration.

In the 1064 nm-excited Raman spectrum (Fig. 4), in the high frequency range, two bands at 1595 and 1555 cm^{-1} are clearly recorded. They correspond to a CC stretching vibration in the ring and a vinyl group CC stretching in doped segments. At low doping level, the band assigned to the CC stretching of the ring (1595 cm^{-1}) in doped segments overlaps with the band due to the ring CC stretching vibration in neutral segments (1582 cm^{-1}). The band located at 1555 cm^{-1} exhibits a shoulder at 1500 cm^{-1} which is coming from that observed at 1546 cm^{-1} in neutral PPV.

Around 1300 cm^{-1}, we observe a triplet at 1329, 1288, and 1268 cm^{-1}. The first band is coming from the mode of CC–H bending of the vinyl group while those located at 1288 and 1268 cm^{-1} are attributed to the interring vibration in the doped segments. These modes originate from those located at 1197 and 1301 cm^{-1} in neutral PPV. In addition, we observe clearly around the band observed at 1178 cm^{-1}, which is assigned to the CC–H bending of the ring, an additional shoulder at 1142 cm^{-1} with this excitation wavelength. The former can originate from the one observed at 1170 cm^{-1} in neutral PPV mode, whereas the latter can be

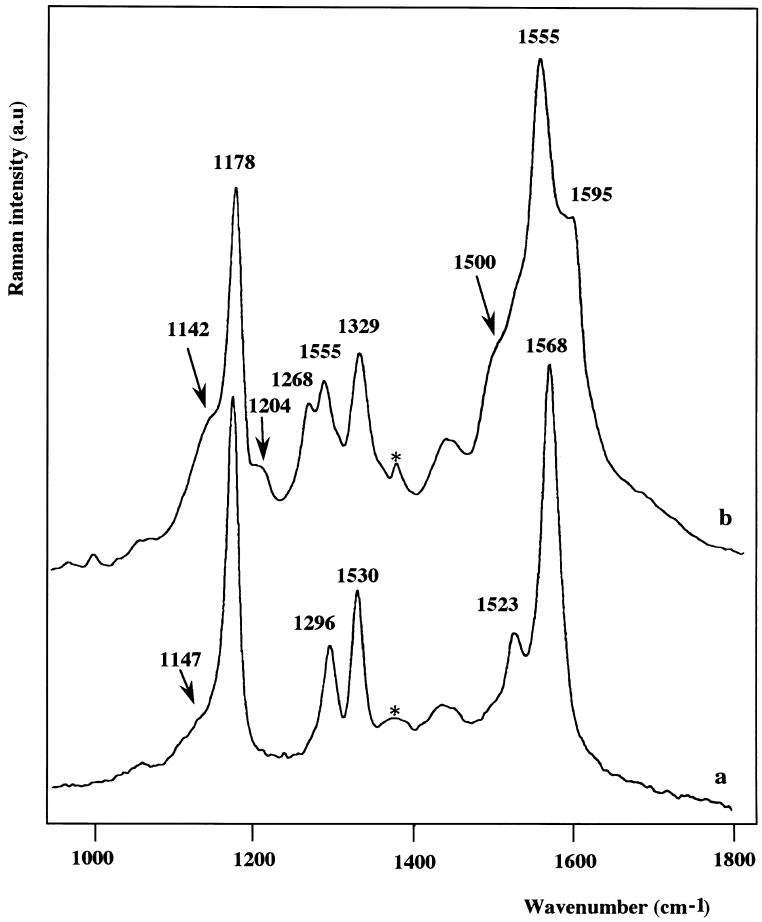

Fig. 5. Raman spectra of BF_4^- doped PPV recorded at 1.3 V with different laser excitation wavelengths: (a) 676.4 nm; (b) 1064 nm; (∗:solvent).

issued to the CC–H bending in doped segments. All the above results are listed in Table 1.

From the above observations, we can confirm the coexistence of different species whose Raman spectra are differently enhanced depending on the excitation wavelength, for the same oxidation level indicating resonance effects. In other words, upon oxidation, different species with different vibrational features are present at low doping level in agreement with optical absorption changes. Considering the Raman bands intensity in the two excitations 676.4 and 1064 nm, one can propose that the bands obtained with 676.4 nm excitation are associated with polarons (maximum absorption at ~2 eV) and those recorded with 1064 nm to bipolarons (maximum absorption at ~0.8 eV).

Therefore, the optical absorption and Resonant Raman spectroscopy coupled to cyclic voltammetry are of main importance to characterize polymeric chain changes induced by doping. Similar effects have been found by Sakamoto [12] with H_2SO_4 doped oligomers using a visible excitation for cations and in near infrared excitation for dications.

The coexistence of these species has been corroborated

Table 1
Assignments and frequencies of polaronic and bipolaronic Raman bands in BF_4^- doped PPV with oxidative potential: 1.3 V/Ag/Ag^+

Neutral PPV (676.4 nm)	Neutral PPV assignments	Polaronic frequencies (676.4 nm)	Bipolaronic frequencies (1064 nm)	p-Doped PPV assignments
1625	Vinylene CC stretch	1605	1595	Ring CC stretch
1582	Ring CC stretch	1568	1555	Vinylene CC stretch
1546	Ring CC stretch	1523	1500	Ring CC stretch
1327	Vinylene CC–H bend	1330	1329	Vinylene CC–H bend
1301	Ring CC–H bend	1296	1288	Inter ring CC stretch
1197	Inter ring CC stretch	1280	1268	Inter ring CC stretch
1170	Ring CC–H bend	1178	1178	Ring CC–H bend
		1147	1142	Vinylene and ring CC–H bend

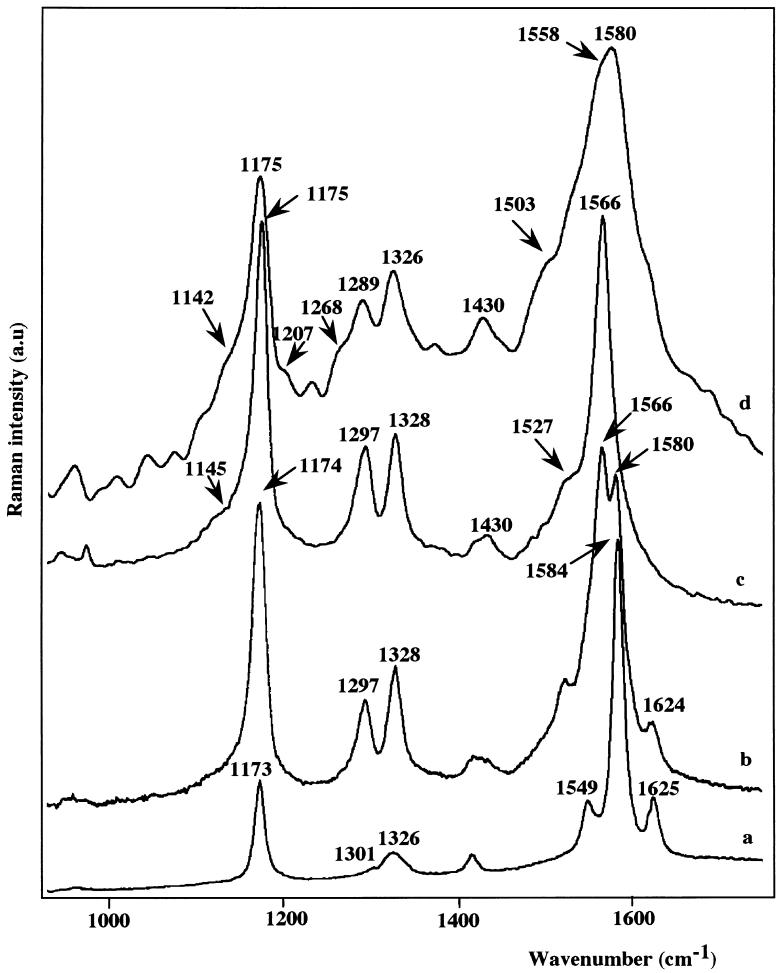

Fig. 6. Raman spectra of SO_3^- overdoped PPV with different laser excitation wavelengths: (a) 457.9 nm; (b) 514.45 nm; (c) 676.4 nm; and (d) 1064 nm (∗:solvent).

by ESR experiments which have partially been published [26]. In situ ESR experiments, designed to follow the creation and annihilation of spins during the electrochemical oxidative doping of PPV have been carried out to determine the ratio spins/charges. We found that this ratio $N_{spins}/N_{charges}$ is much less than one. From this result, we can suggest the predominance of the diamagnetic species. A similar behavior has been obtained previously with oxidized oligomers of PPV and PTV [27]. Our results clearly show the coexistence of polarons and bipolarons in electrochemically oxidized PPV, which are associated to the lattice distortion to a quinoid structure.

3.2. Chemical doping

Raman spectra of SO_3^- doped PPV have been recorded with different doping levels and excitation wavelengths in the visible and near infrared. Raman spectra of lightly doped PPV are similar to that of neutral PPV. Also, at this doping level, it is impossible to obtain spectra with 457.9 and 514.5 nm excitation wavelengths, owing to the important photoluminescence as in neutral PPV.

Raman spectra of highly and overdoped PPV have been obtained with excitation wavelengths in the visible and near infrared, namely 457.9, 514.5, 676.4 and 1064 nm. Notice that there is no significant difference between the Raman frequencies of highly and overdoped PPV but the Raman bands are slightly broadened in the latter case. Thus, we present only the Raman data of the overdoped PPV.

The overdoped PPV Raman spectra with different excitation wavelengths are shown in Fig. 6. According to the excitation wavelengths, the Raman spectra exhibit more or less remarkable changes by comparison to that of neutral PPV.

The 457.9 nm excited Raman spectrum is mostly characteristic of neutral PPV. The main Raman bands are experimentally observed at the following frequencies: 1625, 1584, 1549, 1327, 1301 and 1173 cm^{-1}. However, the upshift of some frequencies and the reverse intensity ratio $I(1625)/I(1549)$ are indicative of short segments. Similar spectra have been observed with the excitation wavelength (363.8 nm) in resonance with short segments in neutral PPV [25,28]. In addition, we observe a small downshift of frequencies as a function of conjugation length as observed

Table 2
Frequencies of polaronic and bipolaronic Raman bands in SO_3^- overdoped PPV

Neutral PPV	Overdoped PPV			
(676.4 nm)	(457.9 nm)	(514.5 nm) Polaronic frequencies	(676.4 nm) Polaronic frequencies	(1064 nm) Bipolaronic frequencies
1625	1625			1580
1582	1584	1566	1566	1558
1546	1549	1524	1527	1503
1327	1327	1328	1328	1326
1301	1301	1294	1297	1289
1197				1268
1170	1173	1174	1175	1175
			1145	1142

in different model compounds with 676.4 nm laser line [29] and 1064 nm one [29,30].

In the 514.5 nm excited Raman spectrum, the main bands are observed at 1624, 1580, 1566, 1524, 1328, 1294 and 1174 cm^{-1}. Raman bands at 1580 and 1624 cm^{-1} are attributed to the presence of neutral segments, even in the SO_3^- overdoped PPV, whereas the other bands in the spectrum are assigned to doped segments. Obviously, the 514.5 nm excited Raman spectrum puts in evidence for the coexistence of doped and neutral segments.

The 676.4 nm excited Raman spectrum shows modifications similar to those obtained with $\lambda_{exc} = 514.5$ nm, except that Raman bands corresponding to the neutral segments are no longer observed. The additional bands are identical to those obtained with electrochemical doping (high potential 1.3 V) indicating that they originate from the same species. Similar spectra have been attributed to the localization of the singly charged defects associated to polarons on the polymeric chain which have a more or less uniform length by comparison with oxidized model compounds [12,31].

The 1064 nm excited Raman spectrum shows a broad Raman band in the 1600 cm^{-1} region. In comparison with the previous modifications of electrochemical oxidized PPV, this band is composed of different components whose frequencies are close to each other. These changes are different to those obtained with 514.5 and 676.4 nm laser lines, owing to resonance effects due to the presence of different species. The changes observed in the 1300 and 1170 cm^{-1} region of frequencies are similar to that obtained with electrochemical doping.

The results presented above are listed in Table 2. They confirm, in good agreement with the previous studies, the coexistence of the polaronic species with neutral segments. Comparatively with electrochemically doped samples, we can suggest, in 1064 nm spectra observed with the former study, the presence of bipolarons in SO_3^- overdoped PPV. However, in view of these results, one can derive that the amount of this species is not important. As a matter of fact, certain defects of the polymer can occur leading to shortened segments and to a decrease in the concentration of

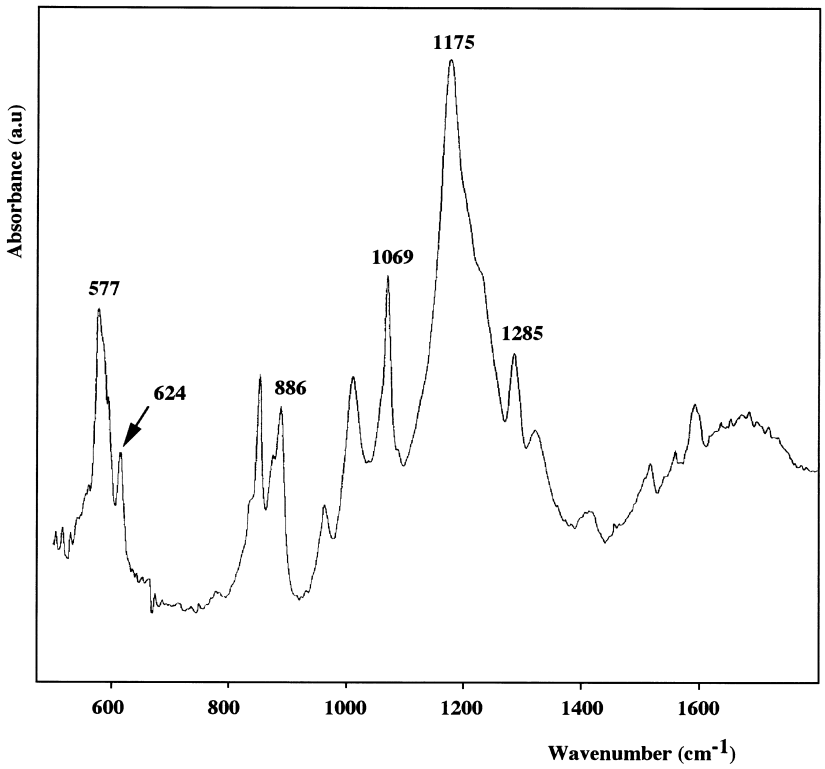

Fig. 7. Infrared spectra of SO_3^- overdoped PPV.

bipolaronic species which can be depicted as fundamental localized excitations responsible for transport properties in conducting polymers with a non-degenerate ground state [27]. This can be related to the lower conductivity of SO_3^- doped PPV by comparison with H_2SO_4 doped PPV [6], and explained by additional covalent bonding. In order to check this, we present in Fig. 7 the infrared spectrum of SO_3^- overdoped PPV. New bands observed at 577, 886, 1069, 1175 and 1285 cm^{-1} are induced by doping. The band observed at 624 cm^{-1} is assigned to the C–S bond, which can also be associated to an overoxidation of the polymeric chain and confirms the shortened conjugation length observed by Raman spectroscopy.

From these studies performed on electrochemically p-doped PPV films, it appears clearly that Raman frequencies are qualitatively more shifted than with Na-doped samples [8]. This puts in evidence for the non-symmetry of polarons and bipolarons in n-doped and p-doped polymer films. This is corroborated by calculations of force constants which will be presented in a forthcoming paper [32]. A possible explanation can be done by invoking steric environment which is basically different in sample doped with BF_4^- or with Na^+. Details are given in Ref. [32].

4. Conclusion

The present study shows that optical absorption spectroscopy and resonant Raman scattering both carried out in situ, and coupled to cyclic voltammetry are useful tools to characterize the different charged defects induced by p-type doping of PPV. In the resonant Raman spectra of doped PPV, a detailed analysis of the Raman bands show clearly that polaronic and bipolaronic species can coexist in p-doped PPV with the predominance of diamagnetic species suggested by in situ ESR electrochemical oxidative doping in the range of the reversible oxidation [27]. The stability of some polaronic segments can also exist in disordered regions [33,34]. The consequences on the structural modifications occurring upon doping are illustrated by the frequency shifts of some Raman bands compared to neutral PPV, when different excitation wavelengths are used. The largest shifts are obtained for the CC stretching modes with 1064 nm laser excitation line. This is in agreement with the presence of a quinoid structure along the PPV chains [35,36]. A lower shift in the frequency of CC stretching modes is recorded with 676.4 nm laser excitation line indicating that a quinoid character structure can be associated to polaronic species [35,36]. On the other hand, compared with sodium doped PPV, the largest shift variation of CC stretching modes seems to indicate a more important distortion of polymeric chain in the case of p-type doping. In the case of chemical doping, Raman results are in each point similar except for the presence of shorter segments presumably due to overoxidation. In order to confirm these experimental results recorded on p-type doping PPV, dynamical calculations performed previously [23] allows, by using the experimental frequencies, a determination of the force constants related to nature of the chemical bonds, and a description of the quinoid-like structure introduced along the polymeric chain after doping [37]. A complete vibration analysis will be presented later [32].

References

[1] Salaneck WR, Lundstrôm, B. Bränby I, editors. Conjugated polymers and related materials New York: Oxford University Press, 1993.
[2] Brédas J-L, Silbey R, editors. Conjugated polymers the novel science and technology of highly conductivity and non linear optically active materials Dordrecht: Kluwer Academic, 1991.
[3] Shirakawa H, Louis EJ, MacDiarmid AG, Chiang CK, Heeger AJ. J Chim Soc Chem Commun 1997;578.
[4] Chiang CK, Fincher CR, Park YW, Heeger AJ, Shirakawa H, Louis EJ, Gau SC, MacDiarmid AG. J Phys Rev Lett 1977;39:1098.
[5] Chiang CK, Druy MA, Gau SC, Heeger AJ, Louis EJ, MacDiarmid AG, Park YW, Shirakawa H. J Am Chem Soc 1978;100:1013.
[6] Murase I, Ohnishi T, Noguchi T, Hirooka M. Synth Met 1987;17:639.
[7] Lefrant S, Buisson J-P, Eckhardt H. Synth Met 1990;37:91.
[8] Orion I, Buisson J-P, Lefrant S. Phys Rev B 1998;57:7050.
[9] Bredas J-L, Themans B, Fripiat JG, Andre JM, Chance RR. Phys Rev B 1984;29:6761.
[10] Obrzut J, Karasz FE. J Chem Phys 1987;87(10):6178.
[11] Onada M, Manda Y, Iwasa T, Nakayama H, Amakawa K, Yoshino K. Phys Rev B 1990;42:11 826.
[12] Sakamoto A, Furukawa Y, Tasumi M. J Phys Chem 1994;98:4635.
[13] Dong Chen MJ, Winokur MA, Masse, Karasz FE. Phys Rev B 1990;41:6759.
[14] Stenger-Smith JD, Lenz RW, Wegner G. Polymer 1989;30:1049.
[15] Wessling RA, Zimmerman RG, US Patent Office, 2, 401, 152 and 3, 706, 677, 1968.
[16] Bradley DDC, Hartmann T, Friend RH, Marzeglia EA, Lindenberger H, Roth S. Springer Ser Solid State Sci 1987;76:308.
[17] Pron A, Genoud F, Nechtschein M, Rousseau A. Synth Met 1989;31:147.
[18] Baïtoul M, Buisson J-P, Lefrant S, Dulieu B, Wéry J, Lapkowski M. Synth Met 1997;84:623.
[19] Krische B, Zagorska M. Synth Met 1989;28:C257.
[20] Bradley DDC, Evans GP, Friend RH. Synth Met 1987;17:651.
[21] Schlenoff JB, Obrzut J, Karasz FE. Phys Rev B 1989;40:11 822.
[22] Voss KF, Foster CM, Smilowitz L, Mihailovic D, Askari S, Srdanov G, Ni Z, Shi S, Heeger AJ, Wudl F. Phys Rev B 1991;43:6.
[23] Buisson JP, Lefrant S, Louarn G, Mevellec JY, Orion I, Eckhardt H. Synth Met 1992;49/50:305.
[24] Mulazzi E, Ripamonti A, Wéry J, Dulieu B, Lefrant S. Phys Rev B 1999;60:16519.
[25] Lefrant S, Perrin E, Buisson J-P, Eckhardt H, Han CC. Synth Met 1989;29:E91.
[26] Baïtoul M, Buisson J-P, Dulieu B, Wéry J, Chauvet O, Lefrant S. J Chim Phys 1998;95:1311.
[27] Bredas J-L, Beljonne D, Shuai Z, Toussaint JM. Synth Met 1991;41–43:3743.
[28] Wéry J, Dulieu B, Bullot J, Baîtoul M, Deniard P, Buisson J-P. Polymer 1999;40:519.
[29] Tian B, Zerbi G, Müllen K. J Chem Phys 1991;95:3198.
[30] Baïtoul M. PhD thesis, Université de Nantes, 1997.
[31] Sakamoto A, Furukawa Y, Tasumi M, Noguchi T, Ohnishi T. Synth Met 1995;69:439.
[32] Baïtoul M, Wéry J, Chauvet O, Buisson JP, Hamdoume M, Lefrant S. In preparation.

[33] Emin D. Phys Rev B 1986;33:6.
[34] Bussac MN, Zupirroli L. Phys Rev B 1994;9:49.
[35] Bredas J-L, Chance RR, Silbey R. Phys Rev B 1982;26:5843.
[36] Eckhardt H, Baughman RH, Buisson J-P, Lefrant S, Cui CX, Kertesz M. Synth Met 1991;41-43:3413.
[37] Lefrant S, Buisson J-P. In: Prasad PN, editor. Frontiers of polymers and advanced materials, New York: Plenum Press, 1994. p. 289–95.